M. MOJŻESZKO[1], K. PERZYŃSKI[1*], M. SIONKOWSKI[1], H. PAUL[2], Ł. MADEJ[1]

NUMERICAL INVESTIGATION OF AN EXPLOSIVE WELDING OF Ti/Cu PLATES BASED ON A MESHFREE METHOD

Development of a reliable numerical model capturing major physical mechanisms controlling explosive welding and considering properties of all process components i.e. base plate and flyer plate is the goal of the paper. To properly replicate materials behavior under these severe conditions a meshfree approach, namely Smooth Particle Hydrodynamics (SPH), was used to discretize the computational domain. The model is based on the Mie-Gruneisen shock equation of state applied to the Ti/Cu system as a case study. Examples of results in the form of velocity, equivalent stress, equivalent strain, and pressure fields are presented within the paper.

Keywords: explosive welding, CEL, SPH, digital material representation

1. Introduction

The application of bi-layered laminar metallic products as construction elements has significantly increased in recent years [1]. Their manufacturing is justified both from the point of view of the fulfillment of specific functional requirements and from an economic perspective. Most often, only a thin layer of material, with elevated functional properties (e.g. with high anti-corrosive properties at higher temperatures), applied on a relatively inexpensive base (construction) material is enough to fulfill the assumed customer's expectations regarding the properties of the final product. A good example of such industrially applicable bi-layered system is a copper/titanium (Cu/Ti) composite. It is often used in electro-technical applications, where low resistivity and high strength, usually in corrosive environments are the main factors affecting the clad applicability. Since it has excellent conductivity it is widely used as busbars for current supply in the galvanizing lines or as anodes in the various electrolysis processes, for example, in cathodes of electrolysers for copper production [2,3]. A variety of methods have been used for the effective joining of Cu and Ti. Most of them are focused on diffusion welding [4], laser welding [5], electron beam welding [6], friction stir welding [7], indirect extrusion [8] or roll-bonding [9]. However, nowadays, it seems that only so called explosive welding opens the possibility to produce large, full-sized plated

coatings of assumed thickness [10]. The concept of this process is schematically presented in Fig. 1.
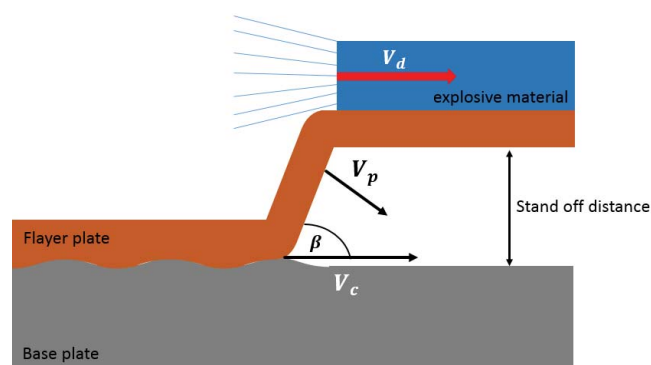

Fig. 1. Schematic illustration of an explosive welding process, β – critical collision angle for a jet formation, V_c – collision velocity, V_p – impact velocity of a flyer plate

As seen in Figure 1, at the collision point, the two surfaces are brought together under a very high pressure. If an impact angle and impact velocity are within the proper range, the high-velocity collision generates a lot of heat leading to a high temperature and also causes high shear strain near the collision point in a very short time. This results in a local melting of the bonded metals which simultaneously initiates local plastic deformation

[1] AGH UNIVERISTY OF SCIENCE AND TECHNOLOGY, DEPARTMENT OF MODELLING AND INFORMATION TECHNOLOGY, AL. A. MICKIEWICZA 30, 30-059 KRAKÓW, POLAND
[2] INSTITUTE OF METALLURGY AND MATERIALS SCIENCE OF POLISH ACADEMY OF SCIENCES, 25 REYMONTA STR., 30-059 KRAKÓW, POLAND

* Corresponding author: kperzyns@agh.edu.pl

near the contact zone [11]. Eventually, a very characteristic wave-like pattern is created along a contact surface (Fig. 2).
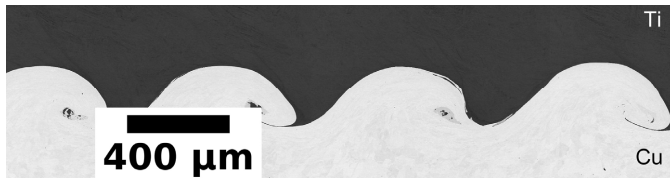

Fig. 2. Wavy surface of the Ti/Cu interface after explosive welding

A very short time of the heat influence, due to the high thermal conductivity of metals, leads to high cooling rates. As a result, in the solidification process, the melted metals are often 'transformed' to be brittle intermetallic of different compounds [12]. At the same time, a work hardening caused by a detonation of an explosive charge provokes series of structural and textural changes that can be observed in the joined metals also in a 'considerable' distance from the bond interface [11]. This heterogeneous distribution of an accumulated strain across both flyer and base plates, and in particular at their bond interface, may adversely affect the behavior of the bi-metal. Therefore, from a scientific point of view, it is worthwhile to analyze and describe changes that occur in this area and especially their relationship with the observed decrease or increase in the properties of the bond.

As presented, explosive welding is an extremely complex process involving various phenomena occurring in materials during a collision at high velocities and pressures, e.g. microstructure changes at very high strain-rates or metallurgical changes occurring at the interfaces of colliding metals. Therefore, to properly understand the material behavior in such conditions a reliable numerical model can be beneficial.

Different numerical approaches have been used in the scientific literature to describe complex physics occurring during explosive welding. The most popular approaches depend on Lagrangian and Eulerian finite element (FE) solutions like ALE (Arbitrary Lagrangian Eulerian). ALE approaches have their advantages and limitations especially when a very dynamic process of explosive welding is considered (see e. g. [13,14]). This technique provides a possibility to take into account general interaction between the two colliding bodies, however, at the same time, it has limitations in the exact identification of the contact point between the two materials. It is also characterized by enormous computing times counted in months, even when modern parallel architectures are used for the simulations. Mesh degeneration during calculations often leads to simulation failure. Therefore, recently in [15] authors have used another variation of mentioned two approaches called CEL (Coupled Lagrangian Eulerian) method and delivered a reasonable description of explosion mechanisms. In the CEL model, it is additionally possible to take into account the interaction between the explosive material and the flyer plate. The mesh degeneration issues are not as severe as in the ALE simulations. However, computing times are still the primary disadvantage of the approach.

The Coupled Eulerian Lagrangian (CEL) model was also previously used by the authors of the current work to investigate the interaction between Ti and Cu plates during explosive welding [16]. In this case, the plate geometries and behavior were described by the classical Lagrangian approach to precisely model interaction between two colliding elements, while explosive material and surrounding air were described by the Eulerian solution to capture gas pressure built up during a high-velocity explosion. Additionally, to describe interactions between explosive pressure wave and flyer plate, the highly refined FE mesh was used. Then, to maintain the computational time at the acceptable level an adaptive multi-level finite element refinement (MLR) algorithm [17] was employed. Additionally, the multi-scale submodelling technique was also used [18,19]. In this case, only a selected part of the sample model was discretized by a high-density FE mesh, while the global model of the process was discretized by a relatively coarse mesh. Examples of obtained interactions between the two colliding plates are shown in Fig. 3.
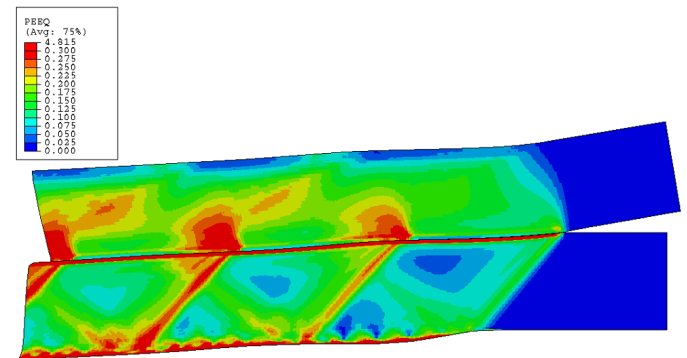

Fig. 3. Equivalent strain recorded along the surface of the flyer and base plates after their collision

As seen in Fig. 3, the simplified 2D CEL model can reasonably predict local deformation state in both plates. However, despite many efforts, it was not possible to recreate the mechanism of generation of the wavy interface.

A rigid nature of finite element meshes seems not to be suitable for problems with such extreme deformation rates. Numerical discrepancies and the amount of computational time required for calculations were the main factors impeding further use of this model for explosive welding simulations.

Therefore, in the present research authors decided to use a different concept introduced by the meshfree methods. Similar approaches have recently been used in the literature to avoid problems with mesh degeneration during flyer and base plates interactions and are very encouraging [20-22]. That is why the Smooth Particle Hydrodynamic method was adapted within the work to investigate its capabilities in predicting plates interactions during a high-velocity collision in explosive welding. To increase the accuracy of the calculation in comparison with the mentioned research, a closed packed highly dense particle cloud was used during the current investigation. The size of the particles directly influences material behavior

especially in the vortex area where material mixing is observed. Therefore, the developed model was discretized with almost 2 500 000 particles, what creates difficulties for sequential calculations due to limitation in the available processing power and enormous computing times. To overcome these issues the multithreaded architecture and parallel computing were used, in the current study, to evaluate capabilities in providing required accuracy in acceptable computing times. The Ti flyer and Cu base plates were selected as a case study for the current investigation.

2. Meshfree model of explosive welding

In the SPH method, the domain is divided into a finite set of nodes often called particles that have defined material properties. Each particle has its own area of influence, which is labeled as a smoothing distance where their properties are smoothed (updated) by a kernel function. This means that the field variables (e.g. density, velocity or pressure) for a single particle within the 3D radius $r = \{x,y,z\}$ are dependent on the other particles in the range of the smoothing distance. This distance is based on a selected smoothing function [23], which introduces a scalar field in the interaction area. The accuracy of the function depends on the defined kernel formula usually represented by a Gaussian type curve.

Material hardening behavior of both flyer and base plates are described by the classical Johnson-Cook hardening rule [16,24]. However, the constitutive formula dealing with the relation between pressure P, density ρ and internal energy E of each system component is described by the Mie-Gruneisen shock equations of state (EoS) [25]:

$$P = P_H + \Gamma \rho (E - E_H) \tag{1}$$

$$\Gamma \rho = \Gamma_0 \rho_0 = constant \tag{2}$$

$$P_H = \frac{\rho_0 c_0 u (1+u)}{\left[1-(s-1)u\right]^2} \tag{3}$$

$$E_H = \frac{1}{2} \frac{P_H}{\rho_0} \left(\frac{u}{1+u}\right) \tag{4}$$

where: E_H – energy at the reference state, Γ – Gruneisen parameter, which represents a thermal pressure from a set of vibrating atoms, Γ_0 – Gruneisen coefficient, ρ – current density, ρ_0 – initial density and c_0 – bulk sound speed.

Mie-Gruneisen EoS parameters used in the current SPH simulations within the LS-Dyna software are gathered in Table 1.

As mentioned in the developed model the flyer (Ti) and base (Cu) plates were modeled with almost 2 500 000 particles. Explosion velocity was recreated by a contact condition and in particular detonation velocity equal to $V_d = 2500$ m/s. The impact velocity V_p is determined by both detonation pressure and stand-off distance between the flyer plate and the base plates. When the flyer plate contacts the base plate at a velocity V_p, a collision angle β remains almost identical for the same stand-off distance. The relationship between the collision angle β, detonation velocity V_d and impact velocity of the flyer plate V_p can be calculated as:

$$V_p = 2V_d \sin\frac{\beta}{2} \tag{5}$$

Two plates with dimensions 30 mm in height and 3mm in thickness as well as the collision angle set to 16° were used as a case study within the investigation. The developed model setup is presented in Fig. 4.
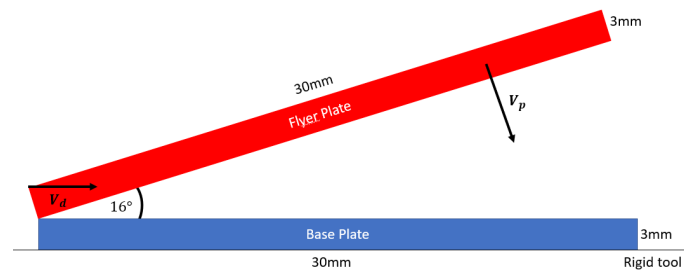

Fig. 4. SPH model setup for an explosive welding simulation

With the application of a large number of particles during the SPH simulation, it should be possible to accurately recreate the jet formation phenomenon and the wavy interface pattern. This was impossible with the earlier FE based attempt. Mechanism of the jet formation is associated with a pressure localized around the collision point. The value of this pressure is much higher than the yield strength of the material. At the same time material near the collision point changes the phase from solid to low viscosity liquid. A jet formation can be divided into three main steps [26]:

a) A jet division into two separate jets: a re-entrant and a salient just after the two plates collide. A single stagnation point that divides these two jets can be identified. Material propelled outside at very high velocity starts to build up as a single hump.

b) A hump formation at the maximal value and stagnation point transfer at the top of the hump. A re-entrant jet moves over the stagnation point and falls down towards a base plate eventually closing the curve.

TABLE 1

Mie-Gruneisen EoS and Johnson-Cook model parameters for titanium and copper [25,26]

Material	ρ_0 [kg/m³]	Γ_0	c_0 [m/s]	s (–)	u (GPa)	A	B	n	m	C
Titanium	4450	1.09	5220	0.767	43	1500	380	0.32	0.7	0.022
Copper	8960	0.75	3940	1.489	98.7	70	292	0.31	1.09	0.025

c) A deformation of the base plate while explosion continues and a repetition of the wave formation. At this time some of the material is ejected by a re-entrant jet and also a new hump begins to form in the front of a new stagnation point.

Examples of initial numerical simulation results (Fig. 5) clearly show a wavy morphology at the interface of the two plates, that clearly prove the capabilities of the developed model and high performance computing environment.
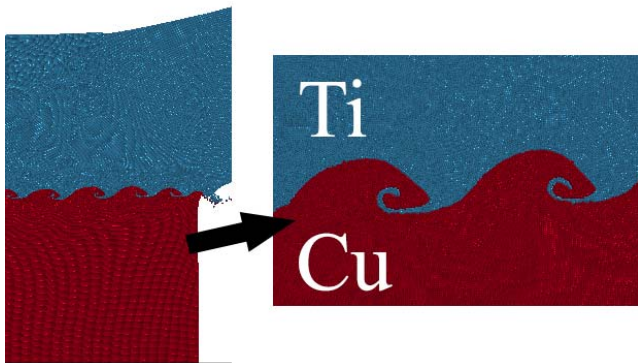

Fig. 5. Wavy morphology at the interface of the Ti and Cu plates after the process

At the same time, the simulation confirms that the highest velocity vectors within the plates are situated at the collision point and reach around 1000 m/s, as seen in Fig. 6.
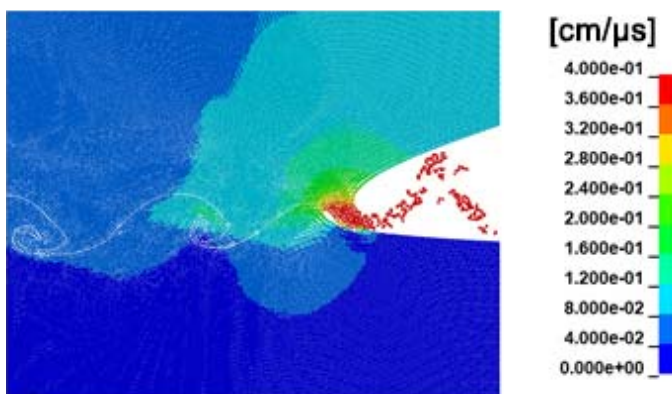

Fig. 6. Velocity at the contact zone during the process

The highest equivalent stress values can be found along the wavy surface. Stress distribution (Fig. 7a) also show that the stresses in the flyer plate are higher than in the base plate, due to different work hardening rates. Equivalent plastic strain (Fig. 7b) within the contact surface of both plates is clearly higher than 2 and pronounced plastic strain gradients across the base plate thickness are also visible.

Important information related to an explosive welding process that can be extracted from the results is also a value of pressure generated between the two colliding plates. During the simulation, the maximum pressure in the collision point reached around 10 GPa as seen in Fig. 8.
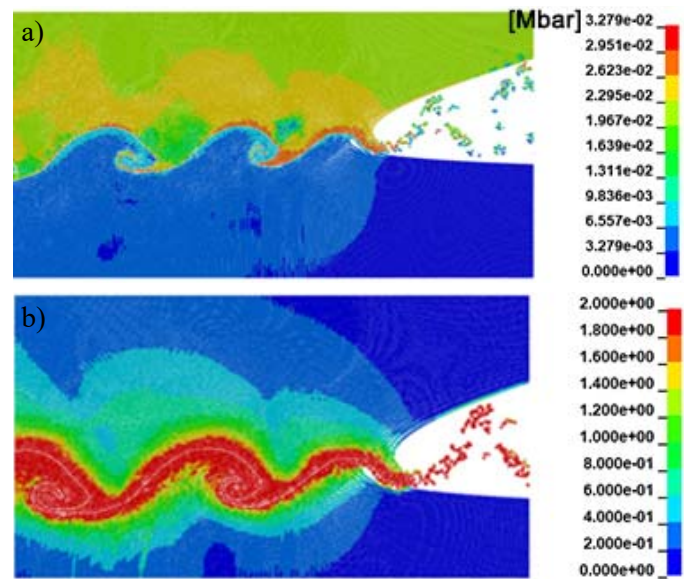

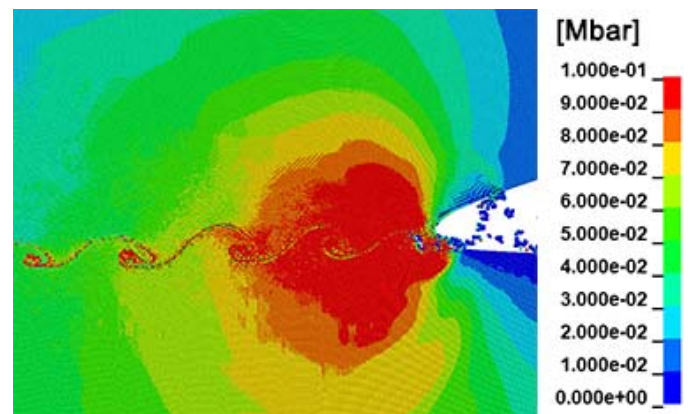Fig. 7. Equivalent stress and strain distribution during the process

Fig. 8. Pressure distribution recorder during the process

As presented, the developed SPH model can qualitatively replicate wavy interface created between the two colliding Cu and Ti plates. Such complex interaction was not possible to recreate by the finite element-based approaches. The model can also recreate the phenomenon of a jet formation, that occurs during the collision at high pressures and velocities. Therefore, the developed numerical model undoubtedly reproduces the formation of a wave-like morphology of the interface with vortexes that are formed just behind the collision point and provides a useful insight into the actual temperature, plastic deformation, stress and pressure distributions in layers near the interface. Obtained results indicate that behind the collision point the high temperature contours are extended along the whole interface and that a melted layer of almost uniform thickness can be formed along the entire contact surface between the sheets. This confirms the hypothesis that solidified melt layer, observed along the boundary of the junction leads to metallurgical bonding between the two plates. Also, the temperature distribution during the clad formation indicates that recrystallization can occur as a result of the heat transfer between the large melted zones and severely

deformed layers of parent sheets. At the same time, the pressure generated at the collision line exceeds the surface forces of the molten material. Therefore, it is clear that molten metals have contributed to the jetting.

Further studies on the model development will be oriented towards quantitative validation of the results by evaluation of wave dimensions predicted numerically and experimentally for various stand-off distances.

3. Conclusions

An explosive welding technique from the numerical point of view is very complex. Extremely short process times and large materials deformations within the thin layers near the interface are very challenging for classical numerical methods involving FE. Many important aspects cannot be captured correctly when standard finite elements are being used. A numerical FE simulation usually requires a large number of elements, that dramatically increases computation time. Numerical approaches like ALE or CEL additionally require a series of remeshing operations to maintain convergence of a solution. As presented, the meshfree SPH method can successfully overcome the mentioned issues. Based on the presented results the following conclusions can be made:

a) Meshfree methods are not constrained by the rigid finite element discretization, thus allowing particles of different materials to blend together. This eventually gives an opportunity to recreate a wavy interface morphology of explosively welded materials.

b) There is no need to reconstruct meshes in case of severe deformations, as particles are not strictly connected. This reduces the computational time.

c) Obtained results in a qualitative manner recreate experimental observations. The temperature, as well as pressure distributions, help to explain local metallurgical phenomena occurring at the plates interface. Further research towards quantitative validation of the developed model is currently undertaken.

REFERENCES

[1] F. Findik, Mater. Des. **32**, 1081-1093 (2011).

[2] A. Sanjurjo, B.J. Wood, K.H. Lau, G.T. Tong, D.K. Choi, M.C.H. McKubre et al., Surf. and Coat. Tech. **49**, 110-115 (1991).

[3] L.Y. Demidenko, N.A. Onatskaya, Surf. Engin. Appl. Electrochem. **44**, 245-247 (2008).

[4] K. Aydın, Y. Kaya, N. Kahraman, Mater. Des. **37**, 356-368 (2012).

[5] Y. Zhao, W. Wang, K. Yan, C. Liu, J. Zou, Jour. of Mat. Proc. Tech. **257**, 244-249 (2018).

[6] S. Guo, Q. Zhou, Y. Peng, X. Xu, C. Diao, J. Kong et al., Mater. Des. **121**, 51-60 (2017).

[7] R. Kumar, M. Balasubramanian, Def. Tech. **11**, 65-75 (2015).

[8] J.S. Lee, H.T. Son, I.H. Oh, C.S. Kang, C.H. Yun, S.C. Lim et al., Jour. of Mat. Proc. Tech. **187-188**, 653-656 (2007).

[9] M. Hosseini, H. Danesh Manesh, Mater. Des. **81**, 122-132 (2015).

[10] H. Paul, W. Skuza, R. Chulist, M. Miszczyk, A. Gałka, M. Prażmowski et al., Metall. and Mat. Trans. A. **51**, 750-766 (2020).

[11] H. Paul, L. Lityńska-Dobrzyńska, M. Prażmowski, Metall. and Mat. Trans. A. **44**, 3836-3851 (2013).

[12] S.A.A. Akbari Mousavi, P. Farhadi Sartangi, Mater. Des. **30**, 459-468 (2009).

[13] A. Nassiri, G. Chini, B. Kinsey, CIRP Annals. **63**, 245-248 (2014).

[14] A. Nassiri, G. Chini, A. Vivek, G. Daehn, B. Kinsey, Mater. Des. **88**, 345-358 (2015).

[15] P.W. Sielicki, T. Łodygowski, Eng. Fail Anal. **104**, 274-291 (2019).

[16] L. Madej, K. Perzynski, H. Paul, Key Eng. Mater. **651-653**, 1415-1420 (2015).

[17] B. Lu, MSc thesis, Conceptual design using multilevel continuum structural topology optimization, University of Iowa, USA (2014).

[18] A.S. Verma, N.P. Vedvik, P.U. Haselbach, Z. Gao, Z. Jiang, Compos. Struc. **209**, 856-878 (2019).

[19] K. Perzyński, A. Wrożyna, R. Kuziak, A. Legwand, L. Madej, Fin. Elem. in Ana. and Des. **124**, 7-21 (2017).

[20] I.A. Bataev, S. Tanaka, Q. Zhou, D.V. Lazurenko, A.M.J. Junior, A.A. Bataev et al., Mater. Des. **169**, 107649 (2019).

[21] Q. Chu, M. Zhang, J. Li, C. Yan, Mat. Sci. and Eng. A. **689**, 323-331 (2017).

[22] Z.L. Zhang, D.L. Feng, M.B. Liu, J. Manuf. Process. **35**, 169-189 (2018).

[23] M.B. Liu, G.R. Liu, K.Y. Lam, Jour. of Comp. and App. Math. **155**, 263-284 (2003).

[24] S.A.A. Akbari Mousavi, S.T.S. Al-Hassani, Mater. Des. **29**, 1-19 (2008).

[25] X. Wang, Y. Zheng, H. Liu, Z. Shen, Y. Hu, W. Li et al., Mater. Des. **35**, 210-219 (2012).

[26] Z.L. Zhang, M.B. Liu, J. Manuf. Process. **41**, 208-220 (2019).